

# Localization by disorder in the infrared conductivity of (Y,Pr)Ba<sub>2</sub>Cu<sub>3</sub>O<sub>7</sub> films

R. P. S. M. Lobo\*

*Laboratoire de Physique du Solide, Ecole Supérieure de Physique et Chimie Industrielles de la Ville de Paris, CNRS UPR 5, 75231 Paris Cedex 5, France*

E. Ya. Sherman

*Institute für Theoretische Physik – Karl-Frazens-Universität, A-8010, Graz, Austria*

D. Racah and Y. Dagan

*Department of Physics and Astronomy – Tel-Aviv University, Ramat-Aviv, Tel-Aviv, 69978 Israel*

N. Bontemps

*Laboratoire de Physique du Solide, Ecole Supérieure de Physique et Chimie Industrielles de la Ville de Paris, CNRS UPR 5, 75231 Paris Cedex 5, France*

(October 28, 2018)

The ab-plane reflectivity of (Y<sub>1-x</sub>Pr<sub>x</sub>)Ba<sub>2</sub>Cu<sub>3</sub>O<sub>7</sub> thin films was measured in the 30–30000 cm<sup>-1</sup> range for samples with  $x = 0$  ( $T_c = 90$  K),  $x = 0.4$  ( $T_c = 35$  K) and  $x = 0.5$  ( $T_c = 19$  K) as a function of temperature in the normal state. The effective charge density obtained from the integrated spectral weight decreases with increasing  $x$ . The variation is consistent with the higher dc resistivity for  $x = 0.4$ , but is one order of magnitude smaller than what would be expected for  $x = 0.5$ . In the latter sample, the conductivity is dominated at all temperatures by a large localization peak. Its magnitude increases as the temperature decreases. We relate this peak to the dc resistivity enhancement. A simple localization-by-disorder model accounts for the optical conductivity of the  $x = 0.5$  sample.

72.15.Rn, 74.25.Gz, 74.76.Bz

## I. INTRODUCTION

The only consensus on the electronic properties of the normal state of high- $T_c$  superconductors is that they are not conventional. Examples of models describing cuprates normal state are charge stripes,<sup>1</sup> polarons,<sup>2,3</sup> various flavors of modified Fermi liquid<sup>4–6</sup> and Luttinger liquid.<sup>7</sup> All these models assume a strong electron-electron and/or electron-phonon interaction. The disorder introduced by cationic or oxygen doping influences the spectrum of excitations making the physics of the system more complex. Indeed, Basov *et al.*<sup>8</sup> propose that the Drude-like peak observed in the infrared spectra of irradiated YBa<sub>2</sub>Cu<sub>3</sub>O<sub>7</sub> (YBCO) moves up in frequency to a localized state. Problems that have been discussed now for many years are the relevance of disorder to localization and localization to superconductivity, in particular near the metal-insulator transition.<sup>9–11</sup> In cuprates, this could apply to a strongly underdoped material. Another twist appears with the observation of a normal state gap in underdoped cuprates.<sup>12–15</sup> It was first observed as a pseudo-gap in NMR data.<sup>16</sup> It was later associated to the departure from linearity in the resistivity.<sup>14,15</sup> Puchkov and coworkers<sup>12</sup> proposed that the apparent optical conductivity spectral weight loss in the normal state of underdoped cuprates is a manifestation of the pseudo-gap.

There is a significant (and somewhat contradictory) body of literature suggesting both hole depletion in

the CuO<sub>2</sub> planes and localization in Pr substituted compounds.<sup>17–25</sup> In this paper we describe the optical reflectivity of Pr doped YBa<sub>2</sub>Cu<sub>3</sub>O<sub>7</sub> (Pr-YBCO) ab-plane thin films as a function of temperature.

The optical conductivity of untwined single crystals of non-superconducting PrBa<sub>2</sub>Cu<sub>3</sub>O<sub>7</sub> shows that substitution of Y by Pr empties the CuO<sub>2</sub> planes and localizes the charges into a mid-infrared band presumably along the CuO chains.<sup>26</sup> Optical<sup>27</sup> ( $x \leq 0.35$ ) and coherent THz<sup>28</sup> ( $x \leq 0.4$ ) data on the in-plane response of Pr-YBCO support a picture in which the localization grows continuously with Pr doping. More recently, Bernhard and co-workers measured the far-infrared c-axis conductivity of Pr-YBCO using ellipsometry. Their data suggest that Pr acts as an underdoping agent.<sup>29</sup> For their highest doping ( $x = 0.45$ ) they find some indirect support of charge localization. However a localization peak has not been resolved in Pr-YBCO.

We investigate Y<sub>1-x</sub>Pr<sub>x</sub>Ba<sub>2</sub>Cu<sub>3</sub>O<sub>7</sub> samples with  $x = 0, 0.4$  and  $0.5$ . The superconducting state of the first two compositions is discussed in detail elsewhere.<sup>30</sup> In this paper we resolve, for the first time, the localization peak in Pr-YBCO at the composition  $x = 0.5$ . A simple localization model based on Pr disorder reproduces this localization peak. We suggest that a signature of this peak is already present in the  $x = 0.4$  compound and competes with the normal state gap opening.

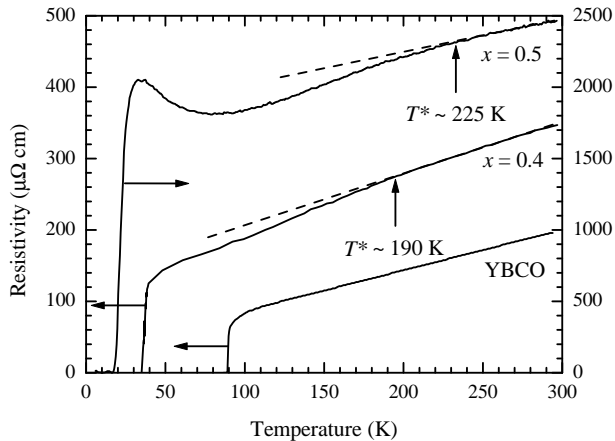


FIG. 1. Temperature dependence of the dc resistivity of (Pr,Y)Ba<sub>2</sub>Cu<sub>3</sub>O<sub>7</sub> films on YSZ. Note that the  $x = 0.5$  compound (right-hand axis) is almost one order of magnitude more resistive than  $x = 0.4$  and pure YBCO. The temperature where the resistivity no longer shows a linear thermal dependence is indicated by  $T^*$ .

## II. EXPERIMENTAL

Thin films of pure and Pr doped YBa<sub>2</sub>Cu<sub>3</sub>O<sub>7</sub> were grown by sputtering on stabilized zirconia (YSZ) substrates. The samples are c-axis oriented and typically 5000 Å thick. The four-point electrical dc resistivity is shown in Fig. 1, giving  $T_c = 90$  K ( $x = 0$ ),  $T_c = 35$  K ( $x = 0.4$ ) and  $T_c = 19$  K ( $x = 0.5$ ). The resistivity of the  $x = 0.5$  compound is almost an order of magnitude higher (right-hand side scale) than that of pure or  $x = 0.4$  Pr YBCO (left-hand side scale). The dashed straight lines help to locate approximately the pseudo-gap opening temperature ( $T^*$ ) in the Pr doped samples, indicated by the arrows. Note that in the  $x = 0.5$  compound an upturn before the superconducting transition occurs. One relevant point to this work is that similar  $T^*$ 's can be seen in underdoped YBCO films<sup>14</sup> having  $T_c$ 's of 70 K and 60 K.

$x$	$T_c$ (K)	$\Omega_p$ (cm <sup>-1</sup> )	$N_{eff}$ (cm <sup>-3</sup> )	$\alpha$ (μΩcm/K)
0	89(1)	22000	$5.1 \times 10^{21}$	0.57
0.4	35(2.5)	19200	$4.1 \times 10^{21}$	0.72
0.5	19(7)	18000	$3.6 \times 10^{21}$	2.3

TABLE I. Pr-YBCO characteristic parameters.  $T_c$  and  $\Delta T_c$  (in parenthesis) are directly obtained from the resistivity in Fig. 1.  $\Omega_p$  and  $N_{eff}$  are obtained with Eq. 2 integrating the room temperature optical conductivity up to 1.5 eV.  $N_{eff}$  uses the bare electron mass as  $m^*$ .  $\alpha$  is the slope of the linear part of the resistivity (dashed lines in Fig. 1).

Our infrared reflectivity spectra were obtained with

a Bruker IFS 66v interferometer between 30 and 7000 cm<sup>-1</sup>. Near-infrared and visible data between 4000 and 30000 cm<sup>-1</sup> were measured in a Cary 4000 grating spectrometer. In the overlapping spectral range, measurements from both spectrometers agree within 0.5 %. We used gold mirrors as a reference for measures in the Bruker spectrometer and silver mirrors in the Cary. We utilized a He gas flow cryostat to measure the spectra between 6 K and room temperature in the whole frequency range. The temperature stability during the measurements was better than 0.5 K.

## III. DATA ANALYSIS

The spectral functions were determined for our samples by Kramers-Kronig transform. At low frequencies (below 30 cm<sup>-1</sup>) a Hagen-Rubens extrapolation was used at all temperatures, including the superconducting state. Above the highest measured frequency (30000 cm<sup>-1</sup>) the reflectivity was assumed to be constant up to 10<sup>6</sup> cm<sup>-1</sup> followed by a  $\omega^{-4}$  termination to infinity. Below 150 K our samples are opaque enough to avoid a significant contribution from the substrate. We also checked that different low frequency extrapolations do not change the conductivities more than 7 % at 100 cm<sup>-1</sup> and not more than 2 % at 200 cm<sup>-1</sup>. Above 250 cm<sup>-1</sup> the differences are negligible in the data of Fig. 1.

A generalization of the Drude model can be obtained using a frequency dependent scattering rate<sup>31,32</sup> defined as

$$\frac{1}{\tau} = \frac{2\pi}{Z_0} \Omega_p^2 \frac{\sigma_1}{\sigma_1^2 + \sigma_2^2}, \quad (1)$$

$Z_0 = 377\Omega$  being the vacuum impedance.  $\Omega_p$ , the effective plasma frequency, is related to the charge density  $n$ , carrier effective mass  $m^*$  and the vacuum permittivity  $\epsilon_0$  by  $\Omega_p^2 = ne^2/\epsilon_0 m^*$ .<sup>33</sup>  $\sigma(\omega) = \sigma_1 + i\sigma_2$  is the complex conductivity.

One can estimate the plasma frequency through the classical sum rule

$$\Omega_p^2 = \frac{Z_0}{\pi^2} \int_0^\infty \sigma_1(\omega) d\omega. \quad (2)$$

One usually introduces a cutoff energy (1–2 eV) in order to restrict the integration to the free carrier contribution. Eqs. 1 and 2 assume that  $\Omega_p$ ,  $\tau^{-1}$  and  $\omega$  are measured in cm<sup>-1</sup> and  $\sigma_1$  in Ω<sup>-1</sup>cm<sup>-1</sup>.

## IV. RESULTS

Fig. 2 shows the real part of the optical conductivity for all three samples:  $x = 0$ , 0.4 and 0.5. The normal state low frequency conductivity extrapolates consistently at various temperatures to the measured dc conductivity (solid symbols).

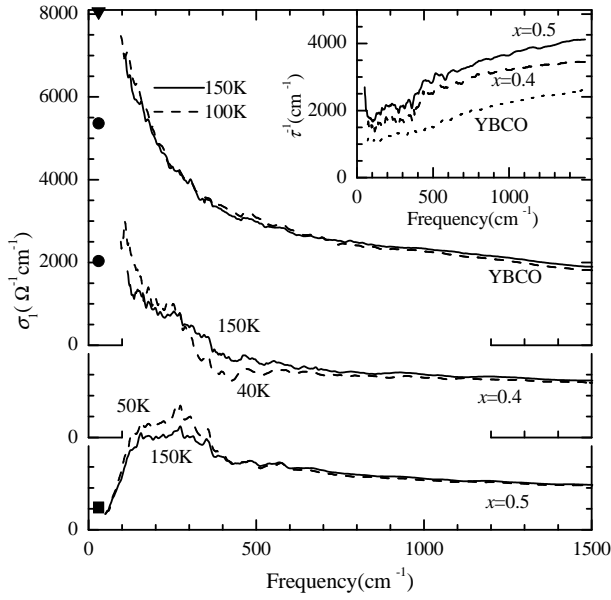


FIG. 2. Real part of the optical conductivity of Pr-YBCO films on YSZ. From top to bottom  $x = 0, 0.4$  and  $0.5$ . The solid symbols are obtained from the dc resistivity for the corresponding temperatures in the normal state. In the  $x = 0.5$  sample  $\sigma_1$  is dominated by a peak around  $250 \text{ cm}^{-1}$ . The inset shows the scattering rate at  $100 \text{ K}$  for all samples. The scales for the  $x = 0.4$  and  $0$  conductivities are shifted with respect to the  $x = 0.5$  sample by  $2000$  and  $4000 \text{ } \Omega^{-1}\text{cm}^{-1}$ , respectively.

The YBCO film exhibits a conventional behavior. Its spectral response does not change significantly in the normal state from  $150 \text{ K}$  to  $100 \text{ K}$  and is dominated by a Drude-like peak. YSZ is not the best substrate to grow YBCO. For instance, the residual conductivity in the superconducting state is twice as high as that from the best films.<sup>30</sup> However, our YBCO's normal state conductivity and scattering rate are qualitatively and quantitatively the same as those from good samples.<sup>12</sup>

In the  $x = 0.4$  film the free carrier response is still the major contribution to the normal state conductivity. The loss of spectral weight from  $\sim 800 \text{ cm}^{-1}$  down to  $300 \text{ cm}^{-1}$  observed at temperatures above  $T_c$  is assigned to the opening of the normal state gap.<sup>30</sup> It is worth remarking at this point that a weak shoulder appears at  $250 \text{ cm}^{-1}$  in the  $40 \text{ K}$  spectrum.

A major change, consistent with the huge increase in the dc resistivity, is observed in the  $x = 0.5$  sample. The free carrier contribution is not seen, and is replaced by a broad peak centered around  $250 \text{ cm}^{-1}$  that dominates the far-infrared spectrum (below  $700 \text{ cm}^{-1}$ ). These spectra do not show any signature of a pseudo-gap or of the superconducting transition. Actually, an opposite effect is observed since the magnitude of the peak around  $250 \text{ cm}^{-1}$  increases with decreasing temperature.

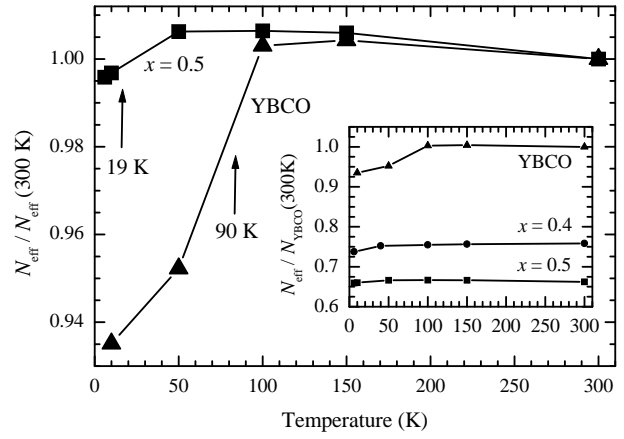


FIG. 3. Thermal dependence of the charge density (normalized to its value at  $300 \text{ K}$ ) calculated with Eq. 2 integrated up to  $1.5 \text{ eV}$ . The arrows indicate the critical temperature for each sample. The estimated error in  $N_{eff}$  is roughly twice the symbol size. The inset shows the same data, now normalized for all samples to the effective charge of YBCO at  $300 \text{ K}$ .

In the inset we show the frequency dependent scattering rate calculated with Eq. 1. The YBCO film displays a standard behavior with a scattering rate  $1/\tau$  depending roughly linearly on frequency in the normal state. In the Pr substituted samples the absolute value of  $1/\tau$  increases and some structures appear at low frequencies ( $250 \text{ cm}^{-1}$ ). Both effects indicate a lower mobility of charge carriers with a possible localization effect.

The values for  $\Omega_p$  estimated from the conductivity integrated up to  $1.5 \text{ eV}$  at  $T = 300 \text{ K}$  are shown in Table I. The charge carrier concentration  $N_{eff}$  is derived from  $\Omega_p$  assuming that  $m^*$  is the bare electron mass. In Fig. 3, we display the thermal evolution of  $N_{eff}$  for each sample normalized by its value at  $300 \text{ K}$ . The estimated error in  $N_{eff}$  is about twice the symbol size. The arrows indicate the measured  $T_c$ . All samples exhibit a decrease of the carrier density when crossing  $T_c$ , associated to the spectral weight transferred to the zero-centered  $\delta$ -function. The inset shows the same data normalized by  $N_{eff}$  of YBCO at  $300 \text{ K}$  for all samples.

## V. DISCUSSION

Even though there are not many data points in Fig. 3, we can infer some general trends for each sample. In pure YBCO we observe that, within experimental error,  $N_{eff}$  does not vary in the normal state. In the  $x = 0.5$  sample  $N_{eff}$  increases when cooling down to  $50 \text{ K}$  and then begins decreasing. The increase is consistent with the accumulating spectral weight in the low frequency peak. The decrease at low temperatures is the signature of the superconducting transition.

The  $x = 0.5$  Pr sample exhibits a clear peak at  $\sim 250$   $\text{cm}^{-1}$ . Experiments in YBCO and pure PBCO have shown a peak in the conductivity when light is polarized along the  $b$  axis.<sup>26,34</sup> In pure PBCO, the peak at an energy  $\sim 1700$   $\text{cm}^{-1}$  has been assigned to localized carriers in the chains.<sup>26</sup> In single domain YBCO crystals, the  $b$ -axis conductivity displays a peak at  $\sim 300$   $\text{cm}^{-1}$ , again assigned to the chains.<sup>34</sup> Other authors did suggest disorder on Pr sites or in oxygen environment.<sup>21,35</sup> 2D localization (hence within the  $\text{CuO}_2$  planes) has also been proposed.<sup>23,35</sup> Localization by disorder is notorious in (superconducting) samples.<sup>36–38</sup> Similar peaks have already been observed in high  $T_c$  compounds,<sup>39–41</sup> some of them being purposely disordered.<sup>8,40</sup> Therefore, we propose to assign this peak to states localized by disorder in our samples, whether in the chains or in the planes.

The influence of Pr ions located between the cuprate planes on the energy of the electronic states in their vicinity has two different reasons. First, Pr changes the energy of the carriers in each  $\text{CuO}_2$  plane. Second, Pr changes the electron hopping matrix element between the planes since the hopping occurs via either Y or Pr orbitals. Due to the hopping the wave functions of the electronic states are either even or odd with respect to the reflection in the Y/Pr plane. The electronic density of the odd states vanishes at the Y/Pr plane, and, therefore, Pr influences the even and the odd states differently. Localization in the planes can be described by a simple quantum mechanical model, a shallow 2D potential well of radius  $a$  and depth  $U_0$ :

$$U(\rho) = \begin{cases} -U_0 & , \rho < a \\ 0 & , \rho \geq a \end{cases}; \quad \frac{\hbar^2}{m^*a^2} > U_0, \quad (3)$$

where  $\rho$  is the in-plane distance. Eq. 3 implies that Pr ions modify in their vicinity the effective crystal potential acting upon the carriers. Therefore,  $2a$  is expected to be close to the lattice parameter in the  $\text{CuO}_2$  plane, while  $U_0$  depends on the parity of the state. The depths of the well should be typically of the order of one eV due to a relatively large difference between Pr and Y ions. However, due to two-dimensionality of the system this potential yields a weakly bound state with the energy  $-\varepsilon_0 \ll U_0$ :

$$\varepsilon_0 = -\frac{2\hbar^2}{m^*a^2} \exp\left(-\frac{2\hbar^2}{m^*a^2} \cdot \frac{1}{U_0}\right), \quad (4)$$

with the Fourier component of the wave function:

$$\psi(q) = 2\sqrt{\pi} \frac{\ell}{1 + \ell^2 q^2}, \quad (5)$$

where the radius of the bound state is  $\ell = \hbar/\sqrt{2m^*|\varepsilon_0|} \gg a$ . An external electric field  $\mathbf{E} = \mathbf{E}_0 e^{-i\omega t}$  ( $\mathbf{E}_0$  being the field amplitude) at the frequency  $\omega \geq -\varepsilon_0/\hbar$  causes transitions from the localized to band states with momentum

$p = \sqrt{2m^*(\hbar\omega + \varepsilon_0)}$ . Using Fermi's Golden Rule, we obtain the transition rate (probability per time unit) from the  $\psi(q)$  state to the band states:

$$W(\omega) = -2\pi\hbar \frac{e^2}{m^*} \varepsilon_0 \frac{\hbar\omega + \varepsilon_0}{(\hbar\omega)^4} f_{\varepsilon_0} (1 - f_{\varepsilon_0 + \hbar\omega}) E_0^2, \quad (6)$$

where  $f_{\varepsilon_0}$  and  $f_{\varepsilon_0 + \hbar\omega}$  are the filling factors of the states. Eq. 6 assumes that the perturbation corresponding to the dipole interaction with the electric field is  $\hat{V} = -i(e/m^*\omega)\hat{\mathbf{p}}\mathbf{E}$ ,  $\hat{\mathbf{p}}$  being the momentum operator. The energy dissipation rate in a medium (per unity volume) is proportional to  $\sigma_1(\omega)E_0^2$ . In other words, the contribution of one localized state to  $\sigma_1(\omega)E_0^2$  is proportional to the energy absorbed per transition multiplied by the transition rate. It then follows that the optical conductivity due to localized states is proportional to  $W(\omega)$  in Eq. 6 multiplied by  $\hbar\omega$  and the concentration of the localized states  $N_L$ . Neglecting the  $\omega$ -dependence of  $f_{\varepsilon_0 + \hbar\omega}$ , the contribution of the localized states with the energy  $\varepsilon_0$  to  $\sigma_1(\omega)$  at  $\omega \geq -\varepsilon_0/\hbar$  is then written as

$$\sigma_L(\omega) = -A\varepsilon_0 \frac{\hbar\omega + \varepsilon_0}{(\hbar\omega)^3}, \quad (7)$$

where  $A$  is a constant proportional to the concentration of the bound states. At a temperature  $T$  a part of the localized states is empty due to thermal excitation, and the thermally activated carriers contribute in the Drude-like way to the optical conductivity. The localized states give the dominant contribution to  $\sigma_1(\omega \sim |\varepsilon_0|/\hbar)$  if  $N_L > N_0 |\varepsilon_0| \tau/\hbar$  for  $|\varepsilon_0| \tau/\hbar \gg 1$  or  $N_L > N_0 \hbar/|\varepsilon_0| \tau$  for  $|\varepsilon_0| \tau/\hbar \gg 1$ , where  $N_0$  is the concentration of the mobile carriers participating in the Drude-like conductivity.

Virtually any conducting oxide shows a broad overdamped mid-infrared band (MIB). Several papers attempted to describe this band in terms of various excitations such as polarons,<sup>42–44</sup> stripes,<sup>45</sup> two magnon,<sup>46</sup> etc. Nevertheless, no conclusive evidence to support any of this effects as being the MIB exists. For any practical purposes, it is widely accepted that the characteristics of the MIB (position and spectral weight) can be obtained from a Lorentz oscillator. Therefore, the general case for the conductivity composed of disordered and mid-infrared states gives

$$\sigma_1(\omega) = \sum_{i=1}^m \sigma_L^{(i)} + \sum_{j=1}^n \frac{2\pi}{Z_0} \frac{\Delta\epsilon_j \Omega_{0(j)}^2 \gamma_j \omega^2}{[\Omega_{0(j)}^2 - \omega^2]^2 + \gamma_j^2 \omega^2}, \quad (8)$$

where the first summation is on disordered states and the second is the Lorentz MIR states.<sup>47</sup>  $\Delta\epsilon$  is the oscillator strength,  $\Omega_0$  is the resonance frequency and  $\gamma$  its damping.

The solid circles in Fig. 4 shows the conductivity of the  $x = 0.5$  sample at 50 K. Since the Pr substitution influences the odd and the even states differently, one expects two different localization energies in the system, which correspond to contribution of the odd and

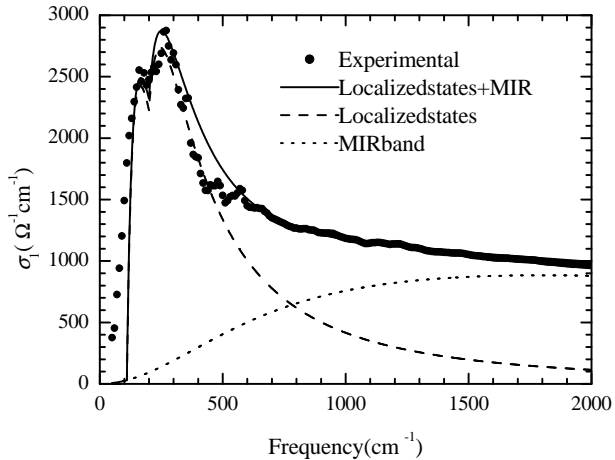


FIG. 4. IR conductivity at 50 K of the  $x = 0.5$  sample. The experimental data are the solid circles. The solid line is composed of two localization peaks and a mid-IR (MIR) peak. The individual contributions of the localization peaks is shown by the dashed line. The dotted line is the MIR contribution.

the even states in  $\sigma_L(\omega)$ . The solid line is a fit using the model in Eq. 8 with two disordered states<sup>48</sup> and one MIR oscillator. Fitting parameters are  $|\varepsilon_0^{(1)}| = 110 \text{ cm}^{-1}$ ,  $A^{(1)} = 1.8 \times 10^6 \Omega^{-1} \text{ cm}^{-2}$ ,  $|\varepsilon_0^{(2)}| = 200 \text{ cm}^{-1}$ ,  $A^{(2)} = 1.5 \times 10^6 \Omega^{-1} \text{ cm}^{-2}$ ,  $\Delta\epsilon = 90$ ,  $\Omega_0 = 1800 \text{ cm}^{-1}$  and  $\gamma = 5500 \text{ cm}^{-1}$ . Individual contributions from disordered localized states and MIR bands are shown, respectively, by dashed and dotted lines. The chosen values for  $A^{(1)}$  and  $A^{(2)}$  correspond to  $N_L \sim 10^{14} \text{ cm}^{-2}$  for odd and even states and  $m^*$  of the order of the bare electron mass. Going back to Eq. 4 we can estimate the radius of the potential well. Since  $a \sim \sqrt{2\hbar}/\sqrt{U_0 m^* \ln(U_0/|\varepsilon_0|)}$ , for  $\varepsilon_0 \sim 200 \text{ cm}^{-1}$  (25 meV) and  $U_0 = 1.0 \text{ eV}$ , we obtain  $a$  close to 2 Å. This radius of the potential well indicates that the changes really happen at the atomic level, consistent with our picture of disorder introduced by Pr ions.

Below  $700 \text{ cm}^{-1}$ , the IR conductivity shown in Fig. 4 is mostly described by this localization model. The model reproduces the amplitude and the asymmetric shape of the localization peak well.<sup>49</sup> The dc conductivity, however, is due to a small free carrier contribution.

Localization reconciles the apparent contradiction between the dc resistivity and the optical conductivity in the  $x = 0.5$  sample. The inset of Fig. 3 shows the behavior of the carrier density  $N_{eff}$  (normalized here to the 300 K YBCO value). The linear parts of the resistivity in Fig. 1 have their slopes shown in Table I. If Matthiessen's law was roughly followed, the ratio between slopes should be proportional to the ratio of the charge densities. The loss in spectral weight for  $x = 0.4$  follows satisfactorily the slope change observed in the dc measurements. The ratio between the resistivity slopes is 0.79 and the inte-

grated charge density of the  $x = 0.4$  compound equals 76 % that from YBCO. This suggests that what we observe here has to be mainly assigned to actual underdoping, namely a decrease of the ratio  $n/m^*$ .

A striking effect appears on the  $x = 0.5$  Pr sample. Whereas its dc conductivity is 5 % of pure YBCO, the integrated carrier density is 65 % of that from YBCO, entirely inconsistent with the observed resistivity increase. The slopes ratio (0.24) is not of much help in solving this puzzle. We are thus led to conclude that the high dc resistivity in the  $x = 0.5$  sample is related to the localization of free carriers rather than to the decrease in their concentration. The Drude-like peak related to mobile charge carriers becomes a peak centered at  $250 \text{ cm}^{-1}$  without a strong loss of spectral weight.

Such a disorder induced localization must build up gradually with Pr concentration and localized states have to be present in the  $x = 0.4$  sample optical conductivity. The frequency dependent scattering rate of the  $x = 0.4$  and  $x = 0.5$  samples show similar structures around  $250 \text{ cm}^{-1}$ . At this very frequency, the optical conductivity of the  $x = 0.4$  material has a shoulder. Thus the localization peak is already present in the  $x = 0.4$  compound. Of course its oscillator strength is smaller and the mobile carriers response dominates the spectra<sup>30</sup> since the conditions  $N_L > N_0 |\varepsilon_0| \tau/\hbar$  or  $N_L > N_0 \hbar/|\varepsilon_0| \tau$  are not yet fulfilled there.

One may remark that the loss of spectral weight in YBCO occurs at all frequencies below  $\sim 800 \text{ cm}^{-1}$ .<sup>12</sup> Why then is the loss of spectral weight in the  $x = 0.4$  material limited to the  $300\text{--}800 \text{ cm}^{-1}$  range? According to the  $x = 0.5$  behavior, the localization peak evolves in the opposite direction of the normal state gap. We suggest that the localization peak in the  $x = 0.4$  sample compensates the normal state gap spectral weight loss in the  $200 \text{ cm}^{-1}$  region thus explaining the apparent discrepancy between underdoped and Pr-substituted YBCO.

## VI. SUMMARY

In summary, the optical response of Pr-YBCO films shows the localization of the charge carriers, thus clearly indicating the coexistence of localization and superconductivity. A peak in the optical conductivity due to this localization effect is fully resolved in the  $x = 0.5$  Pr-YBCO at  $250 \text{ cm}^{-1}$ . We argue that such a localization is already present in the  $x = 0.4$  sample and compensates the normal state gap spectral weight loss. The localization peak is described through in-plane disorder introduced by Pr atoms.

## ACKNOWLEDGMENTS

The authors are grateful to G. Deutscher and R. Combescot for helpful comments, and to B. Briat for his help with the visible measurements. One of us (RPSML) acknowledges the financial support of the UE grant # 93.2027.IL. EYS acknowledges support from the Austrian Science Fund via the project M591-TPH. This work was partially supported by the Oren Family chair of Experimental Solid State Physics.

- 
- \* Present address: LURE – Univ. Paris-Sud – BP 34 – 91898 Orsay Cedex – France – e-mail: lobo@lure.u-psud.fr
- <sup>1</sup> N.L. Wang, A.W. McConnell, and B.P. Clayman, *Phys. Rev. B* **60**, 14883 (1999).
  - <sup>2</sup> M.J. Rice, and Y.R. Wang, *Phys. Rev. B* **36**, 8794 (1997).
  - <sup>3</sup> S.Y. Tian, and Z.X. Zhao, *Physica C* **170**, 279 (1990).
  - <sup>4</sup> C.M. Varma, P.B. Littlewood, S. Schmitt-Rink, E. Abrahams, and A.E. Ruckenstein, *Phys. Rev. Lett.* **63**, 1996 (1989).
  - <sup>5</sup> J.C. Phillips, *Phys. Rev. B* **43**, 3656 (1991).
  - <sup>6</sup> J. Ruvalds, and A. Virosztek, *Phys. Rev. B* **43**, 5498 (1991).
  - <sup>7</sup> M. Ogata, and P.W. Anderson, *Phys. Rev. Lett.* **70**, 3087 (1993).
  - <sup>8</sup> D.N. Basov, A.V. Puchkov, R.A. Hughes, T. Strach, J. Preston, T. Timusk, D.A. Bonn, R. Liang, and W.N. Hardy, *Phys. Rev. B* **49**, 12165 (1994).
  - <sup>9</sup> A. Kapitulnik, and G. Kotliar, *Phys. Rev. Lett.* **54**, 473 (1985).
  - <sup>10</sup> C. Huscroft, and R.T. Scalettar, *Phys. Rev. Lett.* **81**, 2775 (1998).
  - <sup>11</sup> M.V. Sadovskii, *Physics Reports* **282**, 225 (1997).
  - <sup>12</sup> A.V. Puchkov, D.N. Basov, and T. Timusk, *J. Phys. Condens. Matter* **8**, 10049 (1996).
  - <sup>13</sup> C. Renner, B. Revaz, J.Y. Genoud, K. Kadowaki, and Ø. Fischer, *Phys. Rev. Lett.* **80**, 149 (1998).
  - <sup>14</sup> B. Wuyts, E. Osquiguil, M. Maenhoudt, S. Libbrecht, Z. X. Gao, and Y. Bruynseraede, *Phys. Rev. B* **47**, 5512 (1993).
  - <sup>15</sup> T. Ito, K. Takenaka, and S. Uchida, *Phys. Rev. Lett.* **70**, 3995 (1993).
  - <sup>16</sup> H. Alloul, T. Ohno, and P. Mendels, *Phys. Rev. Lett.* **63**, 1700 (1989).
  - <sup>17</sup> J. Fink, N. Ncker, H. Romberg, M. Alexander, M.B. Maple, J. J. Neumeier, and J.W. Allen, *Phys. Rev. B* **42**, 4823 (1990).
  - <sup>18</sup> A.P. Reyes, D. E. MacLaughlin, M. Takigawa, P. C. Hammel, R. H. Heffner, J. D. Thompson, and J. E. Crow, *Phys. Rev. B* **43**, 2989 (1991).
  - <sup>19</sup> D.P. Norton, D.H. Lowndes, B.C. Sales, J.D. Budai, B.C. Chakoumakos, and H.R. Kerchner, *Phys. Rev. Lett.* **66**, 1537 (1991).
  - <sup>20</sup> A.I. Liechtenstein, and I.I. Mazin, *Phys. Rev. Lett.* **74**, 1000 (1995).
  - <sup>21</sup> C.H. Booth, F. Bridges, J. B. Boyce, T. Claeson, Z. X. Zhao, and P. Cervantes, *Phys. Rev. B* **49**, 3432 (1994).
  - <sup>22</sup> A.G. Sun, L.M. Paulius, D.A. Gajewski, M.B. Maple, and R.C. Dynes, *Phys. Rev. B* **50**, 3266 (1994).
  - <sup>23</sup> G.A. Levin, T. Stein, C.C. Almasan, S.H. Han, D.A. Gajewski, and M.B. Maple, *Phys. Rev. Lett.* **80**, 841 (1998).
  - <sup>24</sup> M. Merz, N. Nucker, E. Pellegrin, P. Schweiss, S. Schuppler, M. Kielwein, M. Knupfer, M.S. Golden, J. Fink, C. T. Chen, V. Chakarian, Y.U. Idzerda, and A. Erb, *Phys. Rev. B* **55**, 9160 (1997).
  - <sup>25</sup> R. Fehrenbacher, and T.M. Rice, *Phys. Rev. Lett.* **70**, 3471 (1993).
  - <sup>26</sup> K. Takenaka, Y. Imanaka, K. Tamasaku, T. Ito, and S. Uchida, *Phys. Rev. B* **46**, 5833 (1992).
  - <sup>27</sup> H.L. Liu, M.A. Quijada, A.M. Zibold, Y.D. Yoon, D.B. Tanner, G. Cao, J.E. Crow, H. Berger, G. Margaritondo, L. Forró, O. Beom-Hoan, J.T. Markert, R.J. Kelly, and M. Onellion, *J. Phys. Condens. Matter* **11**, 239 (1999).
  - <sup>28</sup> R. Buhleier, S.D. Brorson, I.E. Trofimov, J.O. White, H.U. Habermeier, and J. Kuhl, *Phys. Rev. B* **50**, 9672 (1994).
  - <sup>29</sup> C. Bernhard, T. Holden, A. Golnik, C.T. Lin, and M. Cardona, *Phys. Rev. B* **62**, 9138 (2000).
  - <sup>30</sup> R.P.S.M. Lobo, N. Bontemps, D. Racah, Y. Dagan, and G. Deutscher, *submitted*.
  - <sup>31</sup> J.W. Allen, and J.C. Mikkelsen, *Phys. Rev. B* **15**, 2953 (1976).
  - <sup>32</sup> For a rather comprehensive review, see A.V. Puchkov, D.N. Basov, and T. Timusk, *J. Phys. Condens. Matter* **8**, 10049 (1996).
  - <sup>33</sup> Written this way,  $\Omega_p$  is a pulsation in MKS units measured in  $\text{s}^{-1}$ . Using the MKS values for  $\epsilon_0$ ,  $e$ ,  $m^*$  and the speed of light  $c$  and taking  $n$  in  $\text{cm}^{-3}$  one obtains the plasma frequency in  $\text{cm}^{-1}$  by  $\Omega_p^2 = 10^{-4} n e^2 / (2\pi c)^2 \epsilon_0 m^*$ .
  - <sup>34</sup> J. Schützmann, B. Gorshunov, K. F. Renk, J. Münzel, A. Zibold, H. P. Geserich, A. Erb, and G. Müller-Vogt, *Phys. Rev. B* **46**, 512 (1992).
  - <sup>35</sup> K. Yoshida, *Phys. Rev. B* **60**, 9325 (1999).
  - <sup>36</sup> P.W. Anderson, K.A. Muttalib, and T.V. Ramakrishnan, *Phys. Rev. B* **28**, 117 (1983).
  - <sup>37</sup> M. Ma, and P.A. Lee, *Phys. Rev. B* **32**, 5658 (1985).
  - <sup>38</sup> A. Kapitulnik, and G. Kotliar, *Phys. Rev. Lett.* **54**, 473 (1985).
  - <sup>39</sup> A.V. Puchkov, T. Timusk, S. Doyle, and A.M. Hermann, *Phys. Rev. B* **51**, 3312 (1995).
  - <sup>40</sup> D.N. Basov, B. Dabrowski, and T. Timusk, *Phys. Rev. Lett.* **81**, 2132 (1998).
  - <sup>41</sup> J.J. McGuire, M. Windt, T. Startseva, T. Timusk, D. Colson, and V. Viallet-Guillen, *Phys. Rev. B* **62**, 8711 (2000).
  - <sup>42</sup> D.M. Eagles, R.P.S.M. Lobo, and F. Gervais, *Phys. Rev. B* **52**, 6440 (1995).
  - <sup>43</sup> S. Lupi, P. Maselli, M. Capizzi, P. Calvani, P. Giura, and P. Roy, *Phys. Rev. Lett.* **83**, 4852 (1999).
  - <sup>44</sup> T. Mertelj, D. Kuščer, M. Kosec, and D. Mihailovic, *Phys. Rev. B* **61**, 15102 (2000).
  - <sup>45</sup> S. Tajima, N.L. Wang, N. Ichikawa, H. Eisaki, S. Uchida, H. Kitano, T. Hanaguri, and A. Maeda, *Europhys. Lett.* **47**, 715 (1999).
  - <sup>46</sup> M. Grüninger, D. van der Marel, A. Damascelli, A. Erb, T. Nunner, and T. Kopp, *Phys. Rev. B* **62**, 12422 (2000).

<sup>47</sup> D.B. Tanner, and T. Timusk, in *Physical Properties of High Temperature Superconductors III*, pp.363-469, Ed. D.M. Ginsberg, World Scientific (1992).

<sup>48</sup> Using a distribution of cutoff energies does not improve the fit, except for rounding the minimum observed between the two peaks. Our best results were obtained with gaussian distributions having widths (FWHM) of 10 and 15  $\text{cm}^{-1}$ . Remarking that the data resolution is 4  $\text{cm}^{-1}$  these distributions are basically single peaks.

<sup>49</sup> As it was shown by W.A. Little [Phys. Rev. A **134**, 1416 (1964)] polarization of localized states can lead to attraction and superconductivity of the carriers. The large polarizability in our case occurs due to the large radius  $\ell$ . Qualitative estimates show that at electron-electron separation less than  $\ell(l/\epsilon a_B)^{1/3}$  the attraction between electrons due to the polarization of the localized states is comparable or larger than their Coulomb repulsion ( $\epsilon$  is the dielectric function, and  $a_B$  is the Bohr radius).